

An exact inversion for anisotropic moduli from phase slowness data

Douglas E. Miller

Schlumberger-Doll Research, Ridgefield, Connecticut

Carl Spencer

Schlumberger Cambridge Research, Cambridge, England

Abstract. The problem of recovering density-normalized elastic moduli of a transversely isotropic anisotropic medium from data consisting of qP or qSV phase velocities measured in multiple directions is addressed. Previous studies have used linear fitting methods with approximate forms of the dispersion relation. Here, it is shown that with algebraic manipulation, and a prior estimate of the squared shear velocity along the symmetry axis (A_{55}), it is possible to use simple linear methods with an exact alternative form of the anisotropic dispersion relation. The method is demonstrated with an application to data from a walkaway vertical seismic profile (VSP) experiment and then used as a tool to address several questions raised by that experiment. It is shown that given data with realistically achievable accuracy, the prior estimate of A_{55} cannot be improved by optimizing the fit to qP data. It is shown that a near perfect fit by a transversely isotropic medium with a vertical symmetry axis (TIV) model to qP data collected in a single vertical plane does not rule out azimuthal anisotropy. Finally, it is shown that a variation of the method, combined with an algorithm suggested by Hood and Schoenberg, suggests a practical way to determine from walkaway VSP data, all the parameters of an orthorhombic medium formed by adding vertical fractures to a transversely isotropic medium.

Introduction

Sedimentary rocks, particularly shales, form principally by the vertical action of gravity and hence are likely to have a fabric that is transversely isotropic, i.e., invariant under rotation around a vertical axis of symmetry. Vertical fractures or the effect of anisotropic horizontal stresses on microcracks can give rise to a medium with lower symmetry, such as an orthorhombic medium (invariant under reflection with respect to each of three mutually orthogonal planes of mirror symmetry). Elastic wave propagation in such media may be expected to show velocity anisotropy, with a phase slowness function that is determined by density, together with an appropriate set of elastic moduli. When analyzing lab data [e.g., Jones and Wang, 1981; Gibson and Toksoz, 1990] or field data [e.g., White *et al.*, 1983; Gaiser, 1990; Miller *et al.*, this issue], researchers may need to find a model to fit a set of phase slowness measurements.

In condensed (Voigt) notation, a homogeneous transversely isotropic medium with a vertical symmetry axis (a "TIV medium") has five independent elastic moduli, c_{11} , c_{13} , c_{33} , c_{55} , c_{66} . The density-normalized moduli, $A_{ij} = c_{ij}/\rho$, have dimensions of squared velocity and, for a homogeneous TIV medium, they are related to elastic propagation as follows. We label the axes interchangeably as 1, 2, 3 or as x , y , z , and we take the z axis as the axis of rotational symmetry. Any plane harmonic wave propagating in the medium, say with phase slowness vector (S_x, S_z) lying in

the x - z plane, must have displacement either in the x - z plane (qP or qSV case) or normal to it (SH case). In either case, the squared phase slowness vector $(X, Z) = (S_x^2, S_z^2)$ must satisfy the appropriate dispersion relation. In the SH case that is

$$A_{66}X + A_{55}Z = 1; \quad (1)$$

and in the qP or qSV case, that is

$$A_{11}A_{55}X^2 + A_{33}A_{55}Z^2 + AXZ - (A_{11} + A_{55})X - (A_{33} + A_{55})Z = -1, \quad (2)$$

where

$$A = A_{11}A_{33} + A_{55}^2 - (A_{13} + A_{55})^2. \quad (3)$$

[cf. Musgrave, 1970, equations (8.1.7) and (8.1.10b)].

For a given set of moduli A_{ij} , equations (1) and (2) implicitly determine X and Z as a function of wave type and propagation direction. We are interested in the inverse problem of determining A_{ij} to best fit a set of measured (squared) phase slownesses $\{(X_i, Z_i): i = 1, n\}$ of known wave type. For the case of SH data, that is straightforward [cf. White *et al.*, 1983]. Equation (1) just becomes an overdetermined linear system

$$A_{66}X + A_{55}Z = 1, \quad (4)$$

$$X = (S_{x_i}^2; i = 1, n), \quad Z = (S_{z_i}^2; i = 1, n),$$

$$\mathbf{1} = (1; i = 1, n)$$

Copyright 1994 by the American Geophysical Union.

Paper number 94JB01848.
0148-0227/94/94JB-01848\$05.00

to be solved for A_{66} and A_{55} by standard methods.

Because (2) is nonlinear in the moduli, determining A_{11} , A_{33} , and A_{13} is more problematical. Previous authors have typically worked with qP data and followed one of three basic approaches:

Method 1

Pick the right three data points [e.g., *Jones and Wang, 1981*]. When X or Z is 0, the left-hand side of (2) factors as a product of simple linear terms. It follows that A_{33} and A_{11} can be determined as the squared qP velocities along and orthogonal to the symmetry axis, respectively. Given a single additional off-axis qP phase slowness measurement (typically at 45°), (2) yields a quadratic expression that can be solved for A_{13} in terms of the measured squared slowness and the other three moduli that affect qP propagation.

Method 2

Use brute force nonlinear methods [e.g., *Gibson and Toksoz, 1990*]. This typically involves making an initial estimate for the moduli, and iteratively calculating (numerically or analytically) Frechet derivatives \mathbf{D} relating change in the measured quantities to changes in the moduli, and revising the estimate by solving a linear system of the form $\mathbf{d} - \mathbf{d}_0 = \mathbf{D}\Delta\mathbf{m}$, where \mathbf{d} are the measured phase slowness points, \mathbf{d}_0 are the phase slowness points generated by the current estimate using (1) and (2), and $\Delta\mathbf{m}$ are the estimated corrections to the moduli. *Hsu and Schoenberg [1993]* used a hybrid of methods 1 and 2, solving directly for the A_{ii} from axial measurements and then using an iterative method to find A_{13} from multiple off-axis qP measurements of group velocity.

Method 3

Use an approximate form of equation (2) [e.g., *White et al., 1983; Gaiser, 1990*]. Assuming that the true model is approximately isotropic, one can obtain approximations to (2) that are linear in parameters that can be related to the moduli. Using linear methods to fit the data with an approximate slowness curve and extracting moduli from the parameters of that curve, one can perform exact forward modeling based on (2) and argue a posteriori that the answer is accurate. This approach can be realized as a special case of method 2 where the initial estimate is isotropic, the Frechet derivatives are calculated analytically, and there is no iteration [cf. *Chapman and Pratt, 1992*].

In the next section, we show that with algebraic manipulation it is possible to use simple linear methods with an exact alternative form of (2). Given a prior estimate for A_{55} , we show that A_{11} , A_{13} , and A_{33} can be determined together, directly from the solution to an appropriate linear system. This method does not require axial qP measurements or assumptions about weak anisotropy. It retains the robustness of linear methods without sacrificing accuracy.

The method described here was used by *Miller et al.* [this issue] to invert qP phase slowness points obtained from walkaway vertical seismic profile (VSP) data by a modified version of the an experimental method described by *Gaiser [1990]*. Carried out in a horizontally stratified offshore environment, the experiment yielded an estimate for A_{55} , together with a set of roughly 200 measurements of qP phase slowness at wide range of inclination angles. The analysis raised several questions which we address in later sections

of the present paper. We show that given data with realistically achievable accuracy, the prior estimate of A_{55} cannot be improved by optimizing the fit to qP data. We show that a near perfect fit by a TIV model to qP data collected in a single vertical plane does not rule out azimuthal anisotropy. Finally, we show that our method, combined with an algorithm suggested by *Hood and Schoenberg [1989]*, suggests a practical way to determine from walkaway VSP data, all the parameters of an orthorhombic medium formed by adding vertical fractures to a TIV medium.

The TI Trick

The qP - qSV dispersion relation (2) can be rewritten

$$A_{11}[A_{55}X^2 - X] + A_{33}[A_{55}Z^2 - Z] + A[XZ] \\ = [A_{55}(X + Z) - 1]. \quad (5)$$

Given (squared) phase data points $\{(X_i, Z_i); i = 1, n\}$ and a value for A_{55} , each of the bracketed quantities becomes a data vector and (5) becomes a linear system similar to (4). In more detail,

$$\begin{aligned} \mathbf{U} &= (A_{55}X_i^2 - X_i; i = 1, n), \\ \mathbf{V} &= (A_{55}Z_i^2 - Z_i; i = 1, n), \\ \mathbf{W} &= (X_iZ_i; i = 1, n), \\ \mathbf{D} &= (A_{55}(X_i + Z_i) - 1; i = 1, n). \end{aligned} \quad (6)$$

Then (5) can be rewritten

$$A_{11}\mathbf{U} + A_{33}\mathbf{V} + A\mathbf{W} = \mathbf{D}, \quad (7)$$

that is, as a linear system to be solved for scalar coefficients A_{11} , A_{33} , and A .

A_{13} can then be obtained directly from (3) assuming $A_{13} + A_{55} > 0$:

$$A_{13} = (A_{11}A_{33} + A_{55}^2 - A)^{1/2} - A_{55}. \quad (8)$$

An alternative solution for A_{13} (with $A_{13} + A_{55} < 0$) would yield a medium with the same phase slowness surfaces, but with anomalous off-axis polarizations [*Helbig and Schoenberg, 1987*]. For inversion of physical measurements, this case is unlikely to occur and can easily be distinguished by looking at polarizations near 45° . Mathematically, it is simply a second solution to the inversion problem which is physically anomalous but is permitted provided certain stability conditions are met [*Helbig and Schoenberg, 1987*, equation (2)].

The only requirement for the applicability of this approach is a prior estimate of A_{55} . Depending on the application and the available set of phase slowness points, this may come from a sonic log, from separate analysis of SH data [*White et al., 1983*], from separate analysis of axial SV data [*Miller et al., this issue*], or it can be treated as a free parameter indexing a family of solutions that can be optimized by a one-parameter search. The method can be applied to any combination of qP and qSV data; however, it should be noted that (5) is degenerate for axial SV points. In the next section we consider applications involving qP points only.

Applications

Inversion of Walkaway VSP Data

Miller *et al.* [this issue] use the above method to invert *qP* phase points obtained from walkaway VSP data by a modified version of the an experimental method described by Gaiser [1990]. A model with density-normalized moduli $\{A_{11}, A_{13}, A_{33}, A_{55}\} = \{6.986, 2.641, 5.527, 0.910\}$ was obtained using 201 input phase slowness points. Units for density-normalized moduli, here and throughout the paper, are km^2/s^2 . For later reference, we call this "model 1."

Figure 1a shows the experimental data points, together with the *qP* phase slowness function from model 1. The model is qualitatively similar to other shale examples [e.g., Jones and Wang, 1981]. It is significantly anisotropic, and the anisotropy is significantly anelliptic. Figure 1b shows the accuracy of the fit to the experimental data, as measured by the percentage relative phase error

$$E[\hat{S}_i, S(\theta_i)] = 100 \frac{\hat{S}_i - S(\theta_i)}{S(\theta_i)},$$

where $\hat{S}_i = (X_i + Z_i)^{1/2}$ is the magnitude of the *i*th measured phase slowness, $\theta_i = \arctan (X_i/Z_i)^{1/2}$ is the associated phase angle, and $S(\theta_i)$ is modeled phase slowness at phase angle θ_i . The root-mean-squared (RMS) error is 0.55%.

For comparison, we inverted the same data using the

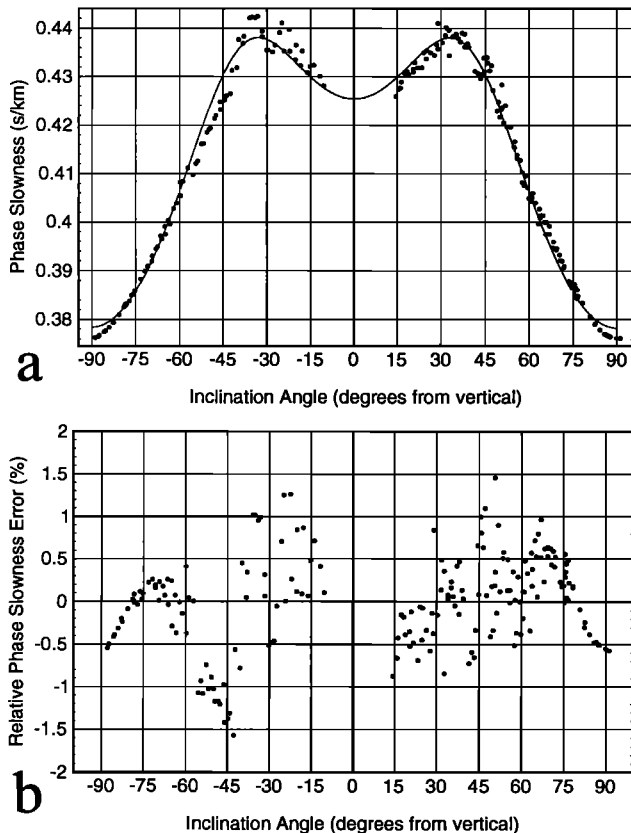


Figure 1. The *qP* phase slowness data from walkaway VSP, fit with an exact slowness function using the method described in the text. (a) Measured phase slowness values and exact slowness function from model 1. (b) Percent relative error of the fit.

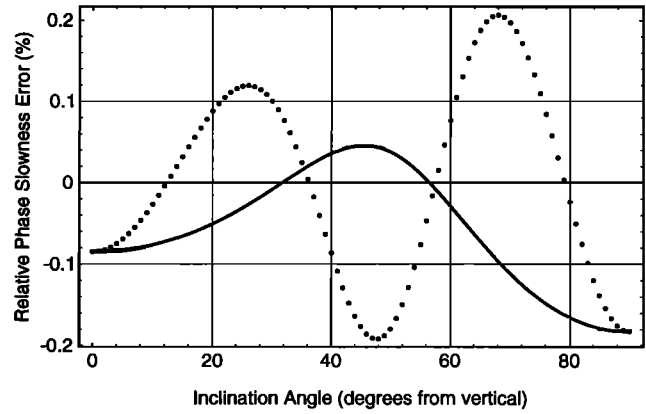


Figure 2. Percent relative phase slowness error in fitting *qP* data from model 1 using the weak anisotropy approximation of Gaiser [1990]. The dotted curve shows errors in the approximating surface. The solid curve shows errors in the exact surface associated with the moduli extracted from the approximation.

approximate method described by Gaiser [1990]. Fitting squared phase velocities using Gaiser's equation (A15) and then converting the approximation coefficients to moduli using his modified (A16) and (A21) (and using the same estimate for A_{55}), we obtained $\{A_{11}, A_{13}, A_{33}, A_{55}\} = \{7.010, 2.601, 5.552, 0.910\}$.

Any method that involves an approximate form of the dispersion relation introduces errors of two types. Type one errors occur because the approximating slowness surface does not fit the exact one. Type two errors occur because the moduli obtained from the approximate surface are incorrect. Figure 2 shows the errors associated with Gaiser's approximation when exact phase data from model 1 were used as input. The dotted curve shows the relative (type one) error $E[S_{\text{app}}(\theta), S(\theta)]$, where $S(\theta)$ are the exact phase values from model 1 and $S_{\text{app}}(\theta)$ are values from the approximating surface. The approximating surface yields density-normalized moduli $m = \{6.998, 2.615, 5.547, 0.910\}$ in this case. The solid curve shows the relative (type two) error $E[S_m(\theta), S(\theta)]$, where $S_m(\theta)$ are exact slowness values for that model. These values are small in comparison with the fitting error shown in Figure 1, so we can conclude that the error introduced by the approximate method is not significant in this case. There is no computational advantage, however, to using the approximate method, and it would be a source of significant error given more accurate measurements.

Poorly Resolved A_{55}

A_{55} is poorly resolved from *qP* data only. Equation (2) involves four parameters $\{A_{11}, A_{13}, A_{33}, A_{55}\}$ that determine the phase surface for *qP* waves, and it is tempting to consider iteratively revising the estimate of A_{55} to optimize the fit. This would allow the determination of all four parameters using *qP* data alone. However, sensitivity analysis based on weak anisotropy [Every and Sachse, 1992; Chapman and Pratt, 1992] shows that for weakly anisotropic media, first-order changes in *qP* phase slowness due to perturbations in $A_{11}, A_{13}, A_{33}, A_{55}$ depend principally upon A_{11}, A_{33} , and the combination $A_{13} + 2A_{55}$. For a medium that is not approximately isotropic, the assumptions of the

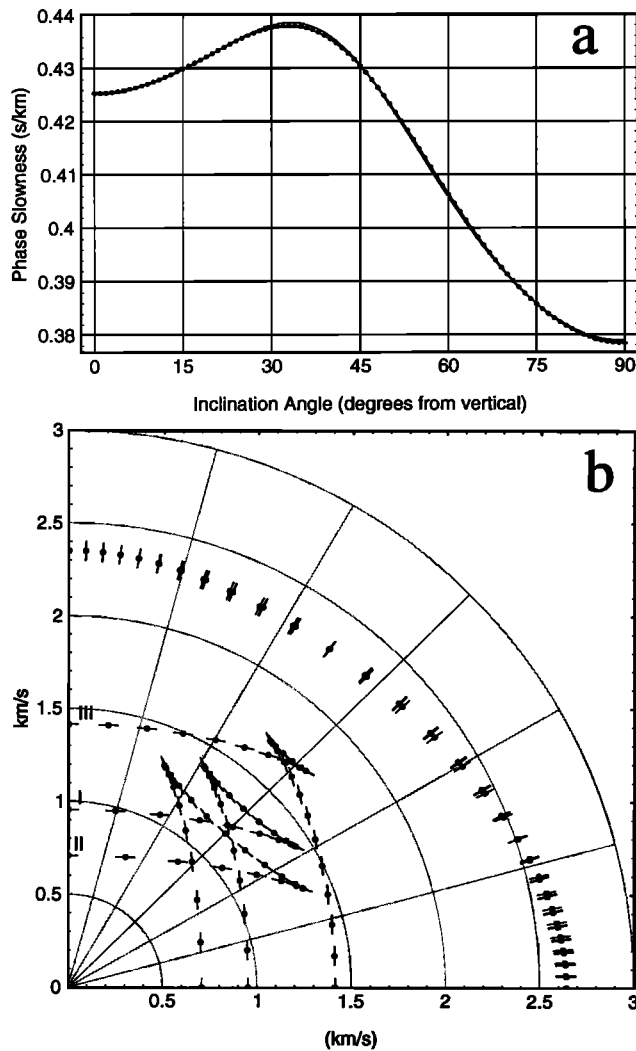


Figure 3. Comparison of three transversely isotropic models. (a) The qP slowness functions. The dotted curve is from model 1. Solid curves are for models 2 and 3. (b) First quadrant group velocity points for models 1–3.

sensitivity analysis do not apply, and it is natural to study sensitivity to A_{55} numerically, using the method described above to vary A_{55} while solving for values of A_{11} , A_{13} , A_{33} in order to fit qP phase slowness points from the original medium. If there is significant variation in goodness of fit as a function of the chosen A_{55} , an estimate of A_{55} could be obtained by a one-parameter optimization. Otherwise, A_{55} must be obtained independently.

We inverted exact qP slowness points from model 1 using values of 0.5 and 2.0 for A_{55} , (that is, with a 100% variation in axial shear velocity), obtaining two media with moduli {6.990, 3.468, 5.526, 0.500} and {6.972, 0.430, 5.530, 2.000} respectively. Below, we refer to these as “model 2” and “model 3.”

Figure 3a shows the qP phase slowness functions for these two media as curves superimposed on the input points created from model 1. RMS variation in the qP phase slowness points between models 2 and 3 is less than 0.1%. Figure 3b shows first quadrant group velocity points for models 1–3. Points are sampled at 3° intervals of phase velocity. The attached tickmarks show the associated polar-

ization direction. The three qP surfaces are effectively indistinguishable, while the qSV surfaces differ dramatically.

Figure 4 shows the relative error as function of the choice of A_{55} used in the inversion, for values of A_{55} ranging from 0.1 to 3.0. Writing $m(a) = \{A_{11}(a), A_{13}(a), A_{33}(a), a\}$ for the medium obtained by inverting using the value a for A_{55} , and $S_{m(a)}(\theta)$ for the associated phase slowness function, the relative phase error $E[S_{m(a)}(\theta), S(\theta)]$ was defined as above, and for each a , the maximum absolute value and RMS average over phase inclination angle, θ , are plotted.

It is difficult to imagine an experiment on a real rock core or subsurface medium that could reduce experimental uncertainty to the level shown in Figure 4 without providing an independent estimate of A_{55} . It is interesting to note that the triplication in the qS surface occurs at all values of A_{55} shown. Thus, while accurate qP measurements do not pin down the value of A_{55} , they can provide a confident qualitative assertion about qSV triplication. The point of interest here is that while the exact shape of the qSV surface cannot be known without knowing A_{55} , large anellipticity in the qP surface implies large anellipticity in the qSV surface, which in turn implies triplication. *Dellinger* [1990] derived an algebraic condition for triplication. See also *Tsvankin and Thomsen* [1992, equation (6)]. It may also be observed that for some applications, all that is required is an accurate representation of the qP surface. In such situations, it would still seem desirable to fit qP data using an exact equivalent of (2), rather than an approximate one.

The values obtained for the moduli as a function of a are well predicted by the weak anisotropy theory, even though the anisotropy here is not weak and the values of A_{55} vary over a wide range. Two theories based on weak anisotropy give similar predictions: $A_{11}(a)$ and $A_{33}(a)$ should be approximately constant, as should either $A_{13}(a) + 2a$ [*Every and Sachse*, 1992; *Chapman and Pratt*, 1992] or $[(A_{13}(a) + a)^2 - (A_{33}(a) - a)^2] / [2A_{33}(a)[A_{33}(a) - a]]$ [*Thomsen*, 1986]. For model 2 these theories predict moduli of {6.986, 3.461, 5.527, 0.500} and {6.986, 3.474, 5.527, 0.500}, respectively. For model 3 they predict {6.986, 0.461, 5.527, 2.000} and {6.986, 0.406, 5.527, 2.000}.

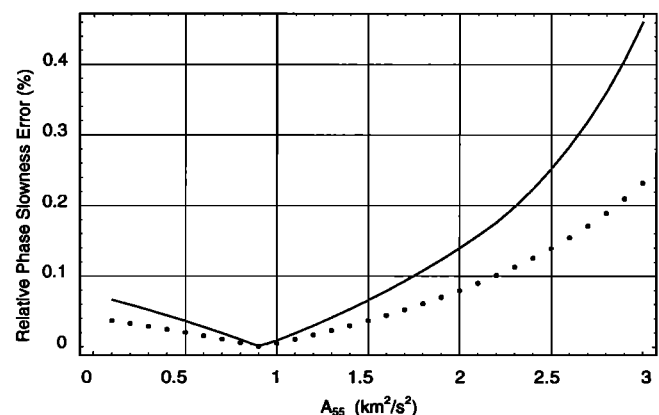


Figure 4. Relative phase slowness error in the qP slowness function as a function of the value of A_{55} used to seed the inversion.

Azimuthal Anisotropy

A good TI fit to data from a single vertical plane does not imply that the medium has negligible azimuthal anisotropy. Model 1 was obtained by fitting a TIV model to *qP* data that were acquired in a single azimuthal plane. It is natural to ask to what extent the good fit by a TIV model can be taken as evidence that the medium is, in fact, TIV. Certainly, the medium is not isotropic, but are there media with lower symmetry than TI that “look TIV” when phase slowness points are sampled in a single randomly chosen vertical plane?

A natural class of models to consider in this regard are the media obtained by adding a fabric of parallel vertical fractures to a TIV medium [Hood and Schoenberg, 1989]. Such media, which we refer to as “fractured TIV” exhibit mirror symmetry with respect to horizontal planes and with respect to vertical planes parallel to and perpendicular to the fractures and are therefore orthorhombic. A general orthorhombic medium has nine independent density-normalized moduli $\{A_{11}, A_{12}, A_{13}, A_{22}, A_{23}, A_{33}, A_{44}, A_{55}, A_{66}\}$. In a fractured TIV medium, the relation

$$A_{22} = \frac{A_{23}}{A_{13}} (A_{11} + A_{12}) - A_{12} \quad (9)$$

holds, reducing the number of independent moduli to eight [Hood and Schoenberg, 1989, equation (13)].

We created a fractured TIV medium by starting with a background TIV medium similar to model 1 with moduli $\{A_{11}^b, A_{13}^b, A_{33}^b, A_{55}^b, A_{66}^b\} = \{7.0, 2.5, 5.5, 1.0, 2.0\}$ and then adding vertical fractures parallel to the 2 axis by the method of Hood and Schoenberg [1989]. Excess compliances $\{\delta_N, \delta_2, \delta_3\} = \{0.10, 0.25, 0.20\}$ were used. The resulting “fractured TIV” medium has moduli

$$A_{ij} = \begin{bmatrix} 6.300 & 2.700 & 2.250 & & & \\ 2.700 & 6.871 & 2.393 & & & \\ 2.250 & 2.393 & 5.411 & & & \\ & & & 1.000 & & \\ & & & & 0.800 & \\ & & & & & 1.500 \end{bmatrix} \quad (10)$$

The *qP* phase slowness values were calculated in this medium for seven azimuths at 0°, 15°, ···, 90° from the 1 axis. (For display purposes in (10), we have rounded the values for A_{22} , A_{33} , and A_{12} to three decimals. Machine-precision numbers were used in the forward calculation.) At each separate azimuth, a best fitting TIV model was obtained using the TI trick. At 0° and 90° the correct vertical shear parameters (0.8 and 1.0, respectively) were used to seed the algorithm. At intermediate azimuths, interpolated vertical shear values between 0.8 and 1.0 were used. Figure 5 shows the seven sets of *qP* phase slowness points with the seven analytic *qP* slowness curves from the TIV models. The models change with azimuth, but the fit at any azimuth is essentially perfect. Figure 6 shows a plot of maximum and RMS misfit as a function of azimuthal angle. In the *x-z* and *y-z* planes, the coupled *qP-qSV* modes satisfy TI dispersion relations [Hood and Schoenberg, 1989] and the fit is perfect. At intermediate azimuths, however, the maximum misfit is less than four parts in 100,000. To rule out a TIV model in practice, given this type of experiment in this type of medium, one must sample multiple azimuths!

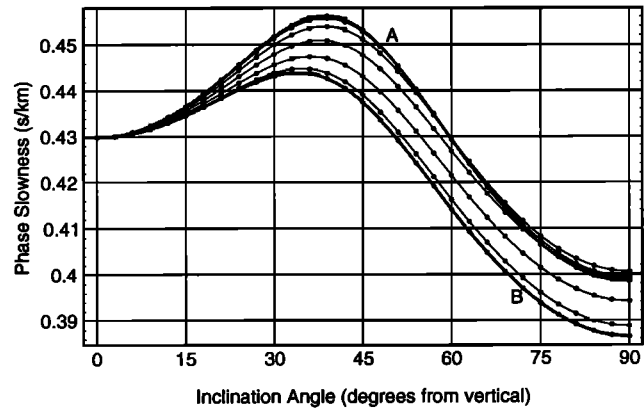


Figure 5. The *qP* phase slowness points at various azimuths for the fractured TIV medium described in the text. At each azimuth a TI medium has been fit to the points, and its phase slowness curve has been superimposed.

Fractured TIV Medium

The TI trick may be used to determine elastic moduli in a fractured TIV medium. Hood and Schoenberg [1989] observed that for a fractured TIV medium (in fact, for any orthorhombic medium) the dispersion relation for phase points lying in any of the symmetry planes has the same algebraic form as (2). (In the *x-z* plane, (2) holds as stated. In the *x-y* plane, change A_{13} to A_{12} and A_{55} to A_{66} ; In the *y-z* plane, change A_{13} to A_{23} and A_{55} to A_{44} .) They suggested that this observation could be exploited to determine the full set of moduli from TI methods applied to data from the symmetry planes. As we now describe it, a modified version of their algorithm can be combined with the TI trick to make a practical scheme for use with walkaway VSP data collected in appropriate azimuthal planes. If the symmetry directions are known in advance, a sufficient data set would involve experiments in the two vertical symmetry planes plus a third at an intermediate azimuth. The following sequence of steps illustrates the algorithm using the example from Figure 5.

Step 1

Identify the symmetry directions and determine A_{55} and A_{44} . This might be done in advance using shear sonic measurements or by examining multiple azimuth walkaway VSP data. Miller et al. [this issue] obtain an estimate for vertical *qSV* slowness in a single azimuth by observing upgoing converted shear waves at near vertical incidence. The *y-z* plane (parallel to the fractures) can be determined from the data in Figure 5 as the azimuth with the minimum *qP* slowness at all inclination angles (in Figure 5 it is curve B). This information could also be obtained from polarization analysis of vertical shear waves (shear splitting) in shear VSP or shear sonic data. If the data are independent of azimuth, then the medium is TIV, and the data can be handled by the method described above. If the medium does not show two orthogonal planes of mirror symmetry, then we are not in an orthorhombic medium and the method does not apply (though it may be of use to find an approximating orthorhombic medium).

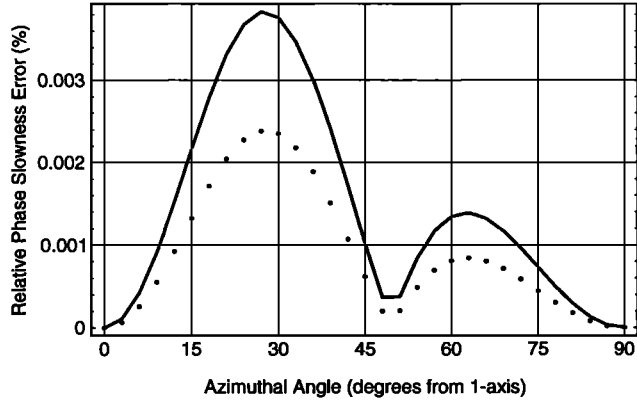


Figure 6. Maximum (solid) and RMS (dotted) percent relative phase slowness error in the best fitting TI *qP* slowness curve as a function of azimuthal angle for the orthorhombic medium described in the text.

Step 2

Use the TI trick to invert the *qP* data in the *x-z* plane for $\{A_{11}, A_{13}, A_{33}, A_{55}\}$ and in the *y-z* plane for $\{A_{22}, A_{23}, A_{33}, A_{44}\}$. These are the models that define curves A and B, respectively, in Figure 5. In our case they are $\{6.300, 2.250, 5.411, 0.800\}$ and $\{6.871, 2.393, 5.411, 1.000\}$, respectively.

Step 3

Solve for A_{12} using equation (9). Equation (9) can be rearranged to solve for A_{12} :

$$A_{12} = (A_{13}A_{22} - A_{11}A_{23}) / (A_{23} - A_{13}). \tag{11}$$

In our example, substituting the values from step 2 into (11), we obtain $A_{12} = 2.684$. This value differs slightly from the correct value (2.700) because the values in step 2 have been rounded to three decimal places and the rounded values do not exactly satisfy (11). Note that (11) is degenerate when the medium is TIV. The accuracy of this method for determining A_{12} increases as the azimuthal anisotropy increases. Using equations (24), (26), and (20) of Hood and Schoenberg [1989], these eight moduli can be converted into seven of the eight parameters that characterize the fractured TIV medium, namely, the five moduli that characterize the background TIV medium plus the normal and vertical shear excess compliances δ_N and δ_3 . In our example, working to three-digit accuracy, we found background moduli $\{A_{11}^b, A_{13}^b, A_{33}^b, A_{55}^b, A_{66}^b\} = \{6.998, 2.499, 5.500, 1.000, 2.008\}$ and excess compliances $\{\delta_N, \delta_3\} = \{0.1, 0.2\}$.

Step 4

Invert a set of at least three *qP* points from the *x-y* plane (the column at 90° in Figure 5) to determine A_{66} . This can be done by using the TIV trick applied to the *x-y* plane *qP* points (as in our first example) to determine A_{12} as a function of A_{66} . This functional relationship can be inverted numerically to find the value of A_{66} that gives the previously determined A_{12} . Figure 7 shows a graph of the best fitting A_{12} as a function of A_{66} , determined using three data points from Figure 5 taken on the *x* axis, on the *y* axis, and at 45° in the *x-y* plane. It is almost a graph of the straight line determined by the equation $A_{12} + 2A_{66} = 5.9$. Thus the added condition $A_{12} = 2.68$ makes a stable, almost linear

problem for determining A_{66} . In our numerical example, we found $A_{66} = 1.508$. Once A_{66} is known, the remaining excess compliance (δ_2) can be calculated directly using equations (20) and (21b) of Hood and Schoenberg [1989]. In our example we found $\delta_2 = 0.249$.

In a more general orthorhombic medium, equation (11) may not hold. If an independent estimate of A_{66} can be made (say, from core measurements), then the horizontal *qP* points can be used to determine A_{12} without appeal to (11) and without need for steps 3 and 4. If only vertical shear points are available and the medium is not far from a fractured TIV medium (in the sense that equation (11) gives a plausible value for A_{12}), then the method described is likely to yield a fractured TIV medium that agrees to experimental accuracy with the true medium at all the measured phase points.

To check this observation, we created phase slowness data as in Figure 5 for a medium with all the A_{ij} as in equation (6), except that for A_{12} , a value of 2.0 was substituted for the original value of 2.7. This new medium has moduli

$$A_{ij} = \begin{bmatrix} 6.300 & 2.000 & 2.250 & & & \\ 2.000 & 6.871 & 2.393 & & & \\ 2.250 & 2.393 & 5.411 & & & \\ & & & 1.000 & & \\ & & & & 0.800 & \\ & & & & & 1.500 \end{bmatrix}. \tag{12}$$

These parameters violate (11) so the resulting medium is not a fractured TIV medium. (Note that we can violate the fractured TIV assumption by changing any one of the moduli occurring in (11) but that a change to any of the axial shear parameters, (A_{44}, A_{55}, A_{66}), would result in a fractured TIV system with a new value for δ_2 or δ_3 .) Inverting as outlined above for a fractured TIV medium and working to machine accuracy, we obtained moduli (rounded here to three decimal places)

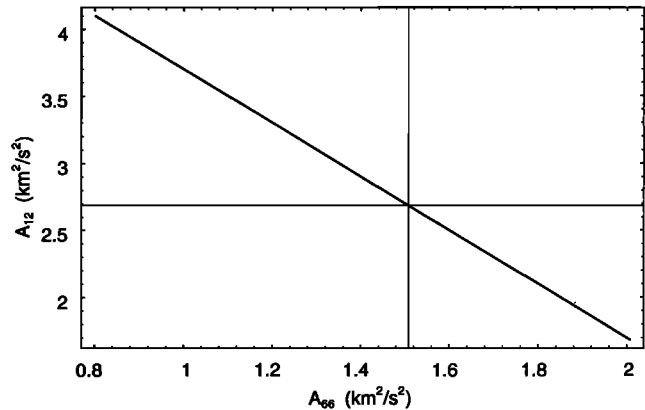


Figure 7. Best fitting A_{12} as a function of A_{66} determined by applying the TI trick to selected *qP* points in the *x-y* plane as described in the text. Horizontal and vertical lines indicate the values $A_{12} = 2.680$ and $A_{66} = 1.508$ determined in the inversion.

